RESEARCH PAPER

Preparation and Characterization of Nanostructured Titania-coated Silica Microsphere Membranes with Simultaneous Photo-catalytic and Water Separation Treatment Applications

V. Tajer-Kajinebaf [1,*], M. Zarrin Khame-Forosh [2] and H. Sarpoolaky [2]

* *vtajer@yahoo.com*

[1] Department of Materials Engineering, Takestan Branch, Islamic Azad University, Takestan, Iran.

[2] School of Metallurgy and Materials Engineering, Iran University of Science & Technology, Tehran, Iran.

Abstract: *In this research, the nanostructured titania-coated silica microsphere (NTCSM) membrane consisting of titania-silica core-shell particles on α–alumina substrate was prepared by dip-coating method. The silica microspheres were synthesized by the Stöber method, and the nanostructured titania shell was obtained from a polymeric sol. Then, the prepared core-shell particles were deposited on alumina substrates. The samples were characterized by DLS, TG-DTA, XRD, FTIR and SEM. The photo-catalytic activity of the NTCSM membranes was evaluated using photo-degradation of methyl orange solution by UV–visible spectrophotometer. In addition, physical separation capability was investigated by filtration experiment based on methyl orange removal from aqueous solution using a membrane setup. The mean particle size of silica microspheres was determined to be around 650 nm, which increased to about 800nm by the deposition of titania nano-particles. After 60 min of UV-irradiation, the dye removal efficiency was determined to be 80% by the membrane. By coupling separation process with photo-catalytic technique, the removal efficiency was improved up to 97%. Thus, the NTCSM membranes showed simultaneous photo-degradation and separation capabilities for dye removal from water.*

Keywords: *Membrane, Nanostructured TiO2, SiO2 microsphere, Titania-silica, Photo-degradation, Separation.*

1. INTRODUCTION

Ceramic membranes have been used in many different industries such as seawater desalination [1-4], biotechnology [5], pharmaceutical [6], feed and beverage [7,8], dairy [9], power generation [10,11] due to stability at high temperatures [12], high pressure and mechanical resistance, good chemical stability, long life and good defouling properties [12,13]. Among them, titania membranes have gained much attention because of their unique characteristics such as chemical stability [14], catalysis [15,16] and their photo-catalytic applications [17-19]. Photo-catalytic activity of titania membranes can be improved by increasing the surface area [20].

Titania particles are not thermally stable and also undergo phase transformation and crystallite growth at high temperatures [21-23]. This phenomenon leads to a reduction in the effective surface area. Deposition of titania particles on a suitable support such as silica in the form of core-shell

particles can be an appropriate method to achieve high surface area. Hence, the core and shell can be formed from the monodisperse silica sphere and titania particles, respectively [24-26]. It seems that deposition and calcination of the titania-silica core-shell particles on ceramic substrates can provide many applications in the field of ceramic membranes with photo-catalytic activity.

According to the author's knowledge, no work has been carried out to produce photo-catalytic membranes via deposition of nanostructured titania-coated silica microsphere particles on α-alumina substrates. In the present work, a sol consisting of titania-silica core-shell particles was prepared by the Stöber method [27]. Then, the obtained sol was deposited on α–alumina substrates by dip-coating process to prepare the nanostructured titania-coated silica microsphere (NTCSM) membranes. The characterization was carried out by dynamic light scattering (DLS), thermogravimetry and differential thermal analysis (TG-DTA), X-ray diffraction (XRD), Fourier transform infrared spectroscopy

(FTIR), scanning electron microscopy (SEM) and UV-Vis spectrophotometer to determine the synthesized membrane properties. Finally, the photo-catalytic and physical separation capabilities of the NTCSM membranes were evaluated via calculation of the methyl orange removal efficiency from aqueous solution by using a dead-end filtration cell equipped with UV-lamp.

2. Experimental procedures

2.1. Materials

The characteristics of the Alumina supports used as the membrane substrate are provided in Table 1.

Table 1. Properties of the used alumina substrate

Composition	α-Alumina
Disk size (mm)	Dia. = 17, Thick. = 2
Pore size (μm)	1-3
Average water absorption (%)	15
Mean open porosity (%)	40

Tetraethyl orthosilicate (TEOS, Merck 800658), ethanol (EtOH, Merck 100983), ammonia (25%, Merck 105432) and deionized water were used as the starting materials for the synthesis of silica microspheres. Titanium tetra-iso-propoxide (TTIP, Merck 821895), isopropanol (IPA, Merck 109634), hydrochloric acid 37% solution (HCl, Merck 100317) and deionized water were used for the preparation of titania polymeric sol. Methyl orange (MO, Merck 101322) with chemical formula of $C_{14}H_{14}N_3NaO_3S$ was used as the model pollutant for the investigation of photo-degradation and physical separation capabilities of the NTCSM membranes.

2.2. Preparation of Membrane

2.2.1. Synthesis of Titania-Coated Silica Microsphere (TCSM)

To prepare titania polymeric sol, a solution of water and HCl in IPA was added dropwise to a solution of TTIP and IPA while stirring vigorous-

ly. The molar ratio of TTIP:IPA:H_2O:HCl in the final sol was 1:31:0.8:0.23, respectively. Finally, a transparent stable titania sol was obtained after stirring for 4h at pH= 0.5. The preparation method of the polymeric titania sol has been described in our previous research [28].

To synthesize silica microspheres using the Stöber method, ammonia was dissolved in a solution of EtOH and water. Then, TEOS was added dropwise to the obtained solution at room temperature. After stirring for 3h, the obtained white precipitate was filtrated and was repeatedly washed with water. Finally, the product was dried at 80 °C for 4h.

To prepare titania–silica core–shell particles, the silica microspheres were dispersed in EtOH. Then, titania polymeric sol was added to this solution. Finally, a sol containing (TCSM) particles was obtained after stirring for 3h at pH= 2.

2.2.2. Deposition of TCSMs on Alumina Substrate

The obtained sol was deposited on the α-alumina substrate by dip-coating method. Also, an unsupported membrane was prepared by pouring the sol in a petri-dish. The supported and unsupported membranes were dried at room temperature for 24h. Then, the samples were heat-treated at 650 °C for 1h at a heating rate of 1 °C/min.

2.3. Characterization

Particle size distribution of the prepared samples was determined by dynamic light scattering technique (DLS Malvern, UK, ZS3600). Thermal behavior of the samples was investigated by thermogravimetry and differential thermal analysis (TG-DTA, PERKINELMER) in a nitrogen atmosphere at a heating rate of 7.5 °C/min. The phase composition was determined by X-ray diffraction technique (XRD, Jeol JDX-8030) with Cu Kα wavelength at 30 mA and 40 kV. Fourier transform infrared spectrometer (FTIR, Bruker, Tensor 27) was used to obtain the infrared spectra of the TCSMs at room temperature on wafers consisting of 100 mg dry KBr and about 1 mg sample. The morphology of the synthesized samples was characterized by scanning electron microscopy (SEM MIRA\\TESCAN) with an accelerating voltage of 20 kV. Also, the photo-catalytic activity of the TCSM membranes was

measured by the photo-degradation of 20 ppm of MO aqueous solution under UV-irradiation source (24 W/cm², 254 nm) by UV-Vis spectrophotometer (Cecil Aquarius, CE 7200). The physical separation experiment was carried out by change in the concentration of MO solution (20 mg/lit) after passing through the TCSM membrane by using a dead-end filtration cell, under a pressure of 5 bar, according to Fig. 1. As shown in this image, to investigate simultaneous separation and photo-catalytic applications of the membranes, filtration cell was equipped with UV-lamp.

Fig. 1. Schematic image of a membrane chamber with a dead-end filtration cell equipped with UV-lamp used for simultaneous separation and photo-catalytic experiments.

3. RESULTS AND DISCUSSION

3.1. DLS

Particle size distribution of the titania polymeric sol, silica spheres and titania-coated silica spheres are given in Fig. 2.
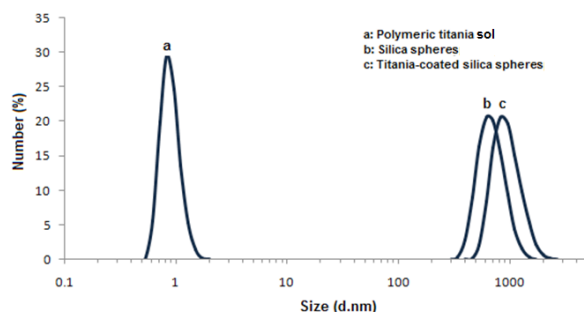

Fig. 2. The particle size distribution of the prepared samples: a) titania polymeric sol, b) silica spheres and c) titania-coated silica spheres.

As shown, the particle size distribution of titania polymeric sol is in the range of 0.5-2 nm with the mean particle size of about 1 nm. Also, the mean particle size of silica spheres is about 650 nm that increases up to 800 nm by the deposition of titania nano-particles. Based on these results, it seems that a layer of titania nano-particles was deposited on silica spheres by physical bonding force (weak Van der Waals force). Thus, the maximum titania shell thickness was found to be about 150 nm.

3.2. DTA/TG

DTA-TG curves of the dried titania gel, silica spheres and titania-coated silica spheres are shown in Fig. 3.

Fig. 3. Thermal analysis of the dried titania gel, silica spheres and titania-coated silica microspheres (TCSM): a) DTA and b) TG curves.

The DTA curves of the samples show an endothermic peak below 150 °C that can be related to the evaporation of the physically absorbed water and solvents. Also, DTA curve of pure titania sample shows a broad exothermic peak in the 200-400 °C range that comes from the decomposition of organic groups, the decomposition of the hydrox-

yl groups as well as titania phase transformation from amorphous to anatase. The DTA curve of the TCSM sample shows two exothermic peaks at 250 and 490 °C. The former may be assigned to the thermal decomposition of organic groups and the latter is related to the phase transformation from amorphous to anatase, although positions and intensities of peaks are strongly dependent on the gel preparation process and its composition [29]. By comparing the DTA curves of silica spheres and TCSM based gels, a relatively small exothermic peak (for TCSM) is observed at about 870 °C, which can be attributed to the phase transition of anatase to rutile [30,31].

According to TG thermographs, the weight loss of the dried titania gel is considerably more than other samples. This behavior is in agreement with the report given in the literature [32]. It can be due to the removal of the remaining organic groups as a result of a partially hydrolyzed alkoxide. The weight loss originates mainly from the removal of physically absorbed water or solvents and organic ligands.

According to TG thermographs, the weight loss of the samples is completed by 650 ºC. Thus, this temperature was considered for calcination of the TCSM membranes.

3.3. XRD

The phase composition of the samples was studied by X-ray diffractometer. Figure 4 shows the XRD patterns of pure titania, silica spheres and TCSMs after calcination at 650 °C.

According to Fig. 4a, the pure silica spheres exhibit amorphous structure at 650 °C. The XRD patterns of the pure titania and TCSMs show a diffraction peak at $2\theta = 25.3°$ that is attributed to anatase crystalline phase [33]. For the pure titania and TCSMs, the anatase crystallite size (calculated by Scherrer's equation [34]) was 21 and 16 nm, respectively. By deposition of titania nano-particles on silica spheres, the peak intensity and crystallite size of anatase phase was decreased. It seems that the deposition of titania on silica spheres delays the phase transformation from amorphous titania to crystalline anatase. This can be attributed to the stabilization of the amorphous phase by the surrounding SiO_2 through the Ti-O-Si interface. The SiO_2 phase locks the Ti–O species at the interface of the TiO_2 domains and prevents the nucleation that is necessary for the phase transformation from amorphous to anatase. Hence, greater heat is required to drive the crystallization [35].

3.4. FTIR

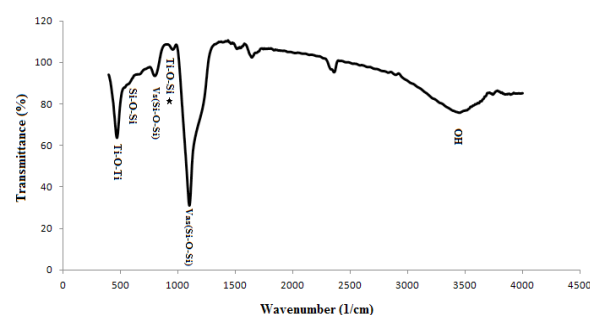FTIR absorption spectrum of the NTCSMs calcined at 650 °C is presented in Fig. 5.

Fig. 4. XRD patterns of the a) silica spheres, b) TCSMs and c) pure titania calcined at 650 °C.

Fig. 5. FTIR absorption spectrum of the NTCSMs calcined at 650 °C.

The broad peak at 3400 cm^{-1} is assigned to O–H groups of absorbed water molecules [36]. Zhijie

Li *et al.* claimed that Ti–O–Ti vibration appears in the range of 400–600 cm^{-1} as a result of condensation reaction [34]. Also, the 800 cm^{-1} peak is assigned to vs (Si–O–Si) symmetric stretching vibration, and the 1087 cm^{-1} peak can be attributed to vas (Si–O–Si) asymmetric stretching vibration, which reveals that a dense silica network is formed. For TiO$_2$-SiO$_2$ core-shell particles, it is possible to distinguish two types of interaction between TiO$_2$ and SiO$_2$: physically mixed (weak Van der Waals forces) and chemically bonded (formation of Ti–O–Si linkages). The IR band at 910–960 cm^{-1} may be due to the stretching vibration of Ti–O–Si bonds [34,37,38]. As a result, the peak at 930 cm^{-1} is attributed to the formation of Ti–O–Si bonds.

3. 5. SEM

SEM images of the silica microspheres as well as the NTCSMs before and after calcination are shown in Fig. 6.

Fig. 6a shows that the synthesized silica particles are spherical in shape with the smooth surfaces. According to this image, the size of silica spheres is in the range of 600-650 nm that is compatible with DLS results. The surface roughness and the increase in the diameter of the silica microspheres in Figs. 6b and 6c confirm that the synthesized spheres have been coated with titania nano-particles. The parameters which affect the formation of NTCSMs are the pH of the solution and so the isoelectric point of TiO$_2$ and SiO$_2$ which causes the charge difference between TiO$_2$ nano-particles and SiO$_2$ microspheres. Isoelectric point of TiO$_2$ and SiO$_2$ is reported to happen in the pH range of 3.9-8.2 and 1.7-3.5, respectively [39-43]. However, a pH equal to 2.0 for the mixed solution is higher than that of the isoelectric point of TiO$_2$ and lower than that of the isoelectric point of SiO$_2$. Therefore, under these conditions TiO$_2$ nano-particles and silica microspheres would have appositive and negative surface charge density, respectively. Thus, titania nano-particles could deposit on the surface of silica microspheres due to the electrostatic attraction between them. As a result, NTCSM particles were produced by the deposition of TiO$_2$ nano-particles on the surfaces of the silica spheres at pH = 2.

Fig. 6. SEM images of a) silica microspheres, b) dried NTCSMs and c) calcined NTCSMs.

Fig. 7 shows the SEM micrographs of the surface and cross-section of the NTCSM membranes. As mentioned, these membranes were prepared by deposition and calcination of the NTCSM sol on the alumina substrate.

Fig. 7. SEM micrographs of the a) surface and b) cross-section of the NTCSM membranes.

As seen in Fig. 7a, the pore size of the NTCSM membrane is less than 400 nm. Also, the thickness of the composite membrane is in the range of 3-4 μm according to Fig. 7b. These images show that the surface of membrane is quite rough at the micrometer scale with a spherical structure. The surface roughness of NTCSM membrane increases its surface area. It can improve photo-catalyt-

ic behavior by increasing the absorption of more photons.

3.6. Photo-Catalytic Experiment

Photo-catalytic activity was determined by the change in concentration of MO aqueous solution under UV-radiation in the presence of the NTCSM membrane. The variation of concentration of MO as a function of the irradiation time was calculated from the absorbance versus concentration calibrated curve. Fig. 8 shows the concentration of MO solution at different times of radiation in the presence of membrane.

Fig. 8. Concentration of MO aqueous solution at the different times of radiation in the presence of the NTCSM membrane.

The removal efficiency of MO was estimated by applying the Eq. (1):

Removal efficiency (%) = [(C_0-C)/C] × 100 (1)

where, C_0 is the original MO concentration and *C* is the residual MO concentration in solution [44].

Fig. 8 indicates that the MO removal efficiency in the presence of the NTCSM membrane is about 80 and 98% after 60 and 120 min of radiation, respectively. In this process, titania nano-particles deposited on silica microspheres absorb the UV-irradiation to generate negatively and positively charged ions, the latter of which interacted with water to produce -OH radicals that degrade the MO. Under this condition, the mechanism of photo-degradation is controlled by the SiO$_2$ spheres in a manner that, the electrons generated from the TiO$_2$

40

shell are immediately pulled towards the internal core. Consequently, the different charges of ions are separated and the productions of the radicals are facilitated. High surface area of particles (as seen in SEM images) increases photo-catalytic activity of the NTCSM membranes.

3.7. Physical Separation Experiment

The dye separation capability by the NTCSM membranes was determined via direct measurement of the change in concentration of MO aqueous solution after passing through membrane at 5 bar pressure during 60 min (see Fig. 1). Fig. 9 compares MO solution concentration before and after passing through the alumina substrate with and without NTCSM layer.

Fig. 9. Concentration of MO solution before and after passing through the membrane substrate with and without NTCSM layer.

Based on the results of physical separation, the MO removal efficiency by the alumina substrate was determined to be 4% which was improved up to 24% in the presence of the NTCSM layer.

3.8. Simultaneous Photo-catalytic and Separation Experiment

By coupling physical separation with photo-catalytic technique (see Fig. 1), the MO removal efficiency was remarkably improved up to 97%, while it was 80% and 24% with any of the photo-catalytic and separation techniques, respectively. Fig. 10 compares MO removal efficiency by the NTCSM membrane via the different techniques.

Fig. 10. MO removal efficiency by the NTCSM membrane via the different techniques.

Thus, the NTCSM membrane showed a high potential due to its multifunctional capability consisting of photo-degradation and physical separation for MO removal from aqueous solution.

4. CONCLUSION

The nanostructured titania-coated silica microsphere (NTCSM) membrane consisting of titania-silica core-shell particles on the α–alumina substrate was prepared by dip-coating process. The silica microspheres were synthesized by the Stöber method, and the nanostructured titania was obtained from a polymeric sol prepared by a hydrolysis–condensation reaction of titanium tetra-isopropoxide precursor. The polymeric titania sol was deposited on silica microspheres based on electrostatic attraction strategy and then, alumina substrates were coated by the prepared NTCSM sol. The mean particle size of silica of microspheres was determined to be about 650 nm that by deposition of titania nano-particles increased up to about 800 nm. The pore size of the NTCSM membrane was determined to be in the range of 100-400 nm with the average thickness of 3.5 μm. The removal efficiency of methyl orange by the NTCSM membrane via photo-catalytic process was determined to be 80% after 60 min UV-irradiation. By coupling separation process with photo-catalytic technique, the removal efficiency was improved up to 97%. Thus, the NTCSM membranes showed simultaneous photo-degradation and separation capabilities for methyl orange removal from aqueous solution.

REFERENCES

1. Kang, J. S., Chang Sung, S., Lee, J. J. and Kim, H. S., "Application of ceramic membrane for seawater desalination pretreatment", Desalination Water Treat., 2016, 1-6.

2. Achiou, B., Elomari, H., Bouazizi, A., Karim, A., Ouammou, M., Albizane, A., Bennazha, J., Alami Younssi, S. and El Amrani, I. E., "Manufacturing of tubular ceramic microfiltration membrane based on natural pozzolan for pretreatment of seawater desalination", Desalination, 2017, 419, 181-187.

3. Xu, J., Chang, C. Y. and Gao, C., "Performance of a ceramic ultrafiltration membrane system in pretreatment to seawater desalination", Sep. Purif. Technol., 2010, 75, 165-173.

4. Gazagnes, L., Cerneaux, S., Persin, M., Prouzet, E. and Larbot, A., "Desalination of sodium chloride solutions and seawater with hydrophobic ceramic membranes", Desalination, 2007, 217, 260-266.

5. Ingham, C. J., ter Maat, J. and de Vos, W. M., "Where bio meets nano: The many uses for nanoporous aluminum oxide in biotechnology", Biotechnol. Adv., 2012, 30, 1089-1099.

6. Svojitka, J., Dvořák, L., Studer, M., Straub, J. O., Frömelt, H. and Wintgens, T., "Performance of an anaerobic membrane bioreactor for pharmaceutical wastewater treatment", Bioresour. Technol., 2017, 229, 180-189.

7. Agana, B. A., Reeve, D. and Orbell, J. D., "Performance optimization of a 5 nm TiO_2 ceramic membrane with respect to beverage production wastewater", Desalination, 2013, 311, 162-172.

8. Agana, B. A., Reeve, D. and Orbell, J. D., "Pre-treatment of beverage production wastewater using a 5 nm TiO_2 ceramic ultrafiltration membrane", Procedia Eng., 2012, 44, 666-669.

9. Kanjwal, M. A., Barakat, N. A. M. and Chronakis, I., "Photocatalytic degradation of dairy effluent using $AgTiO_2$ nanostructures/polyurethane nanofiber membrane", Ceram. Int., 2015, 41, 9615-9621.

10. Dong, X. and Jin, W., "Mixed conducting ceramic membranes for high efficiency power generation with CO_2 capture", Curr. Opin. Chem. Eng., 2012, 1, 163-170.

11. Hashim, S. S., Mohamed, A. R. and Bhatia, S., "Oxygen separation from air using ceramic-based membrane technology for sustainable fuel production and power generation", Renew. Sustainable Energy Rev., 2011, 15, 1284-1293.

12. Sekulic, j., Ten Elshof, J. E., and Blank, D. H. A., "Synthesis and characterization of microporous titania membranes", J. Sol-Gel Sci. Technol., 2004, 31, 201-204.

13. Ju, X., Huang, P., Xu N. and Shi, J., "Studies on the preparation of mesoporous titania membrane by the reversed micelle method", J. Member. Sci., 2002, 202, 63-71.

14. Wang, Y. H., Tian, T. F., Liu, X. Q. and Meng, G. Y., "Titania membrane preparation with chemical stability for very hash environments applications", J. Member. Sci., 2006, 280, 261-269.

15. Hyun, S. H. and Kang, B. S., "Synthesis of titania composite membranes by the pressurized sol-gel technique", J. Am. Ceram. Soc., 1996, 79, 279-282.

16. Bet-moushoul, E., Mansourpanah, Y., Farhadi, Kh. and Tabatabaei, M., "TiO_2 nanocomposite based polymeric membranes: a review on performance improvement for various applications in chemical engineering processes", Chem. Eng. J., 2016, 283, 29-46.

17. Alem, A., Sarpoolaky, H. and Keshmiri, M., "Sol–gel preparation of titania multilayer membrane for photocatalytic applications", Ceram. Int., 2009, 35, 1837-1843.

18. Alem, A., Sarpoolaky, H. and Keshmiri, M., "Titania ultrafiltration membrane: Preparation, characterization and photocatalytic activity", J. Eur. Ceram. Soc., 2009, 29, 629-635.

19. Tajer-Kajinebaf, V., Sarpoolaky, H. and Mohammadi, T., "Synthesis of nanostructured anatase mesoporous membranes with photocatalytic and separation capabilities for water ultrafiltration process", Int. J. Photoenergy, 2013, Article ID 509023, 2013, 1-11.

20. Tajer-Kajinebaf, V., Sarpoolaky, H. and Moham-

madi, T., "Sol–gel synthesis of nanostructured titania–silica mesoporous membranes with photo-degradation and physical separation capacities for water purification", Ceram. Int., 2014, 40, 1747-1757.

21. Kamaruddin, S. and Stephan, D., "The preparation of silica–titania core–shell particles and their impact as an alternative material to pure nano-titania photocatalysts", Catal. Today, 2011, 161, 53-58.

22. Tajer-Kajinebaf, V. and Sarpoolaky, H., "Rapid synthesis of nanostructured pure anatase TiO$_2$ with high thermal stability by polymeric sol-gel route", Journal of Ultrafine Grained and Nanostructured Materials, 2013, 46, 39-45.

23. Chen, Y. F., Lee, C. Y., Yeng, M. Y. and Chiu, H. T., "The effect of calcination temperature on the crystallinity of TiO$_2$ nanopowders", J. Cryst. Growth, 2003, 247, 363-370.

24. Lee, J .W., Kong, S., Kim, W. S. and Kim, J., "Preparation and characterization of SiO$_2$/TiO$_2$ core-shell particles with controlled shell thickness", Mater. Chem. Phys., 2007, 106, 39-44.

25. Huang, H., Sun, A., Zhang, J., Wang, B., Chu, C., Li, Y. and Xu, G., "Facile synthesis of silica–titania core–shell microsphere and their optical transmission spectra", Mater. Lett., 2013, 110, 260-263.

26. Kalele, S., Dey, R., Hebalkar, N., Urban, J., Gosavi, S. W. and Kulkarni, S. K., "Synthesis and characterization of silica-titania core-shell particles", PRAMANA- J. Phys., 2005, 65, 787-791.

27. Stöber, W. and Fink, A., "Controlled growth of monodisperse silica spheres in the micron size range", J. Colloid Interface Sci., 1968, 26, 62-69.

28. Tajer-Kajinebaf, V., Sarpoolaky, H. and Mohammadi, T., "Comparative study on properties of nanostructured titania synthesized by colloidal and polymeric sol gel routes", Iranian Journal of Materials Science & Engineering, 2013, 10, 28-38.

29. Yu, J., Zhao, X. and Zhao, Q., "Effect of surface structure on photo-catalytic activity of TiO$_2$ thin films prepared by sol-gel method", Thin Solid Films, 2000, 379, 7-14.

30. Zhao, L., Yu, J. and Cheng, B., "Preparation and characterization of SiO$_2$/TiO$_2$ composite microspheres with microporous SiO$_2$ core/mesoporous TiO$_2$ shell", J. Solid State Chem., 2005, 178, 1818-1824.

31. Yu, J., Zhao, L. and Cheng, B., "Facile preparation of monodispersed SiO$_2$/TiO$_2$ composite microspheres with high surface area", Mater. Chem. Phys., 2006, 96, 311-316.

32. Khalil, K. M. S., Elsamahy, A. A. and Elanany, M. S., "Formation and characterization of high surface area thermally stabilized titania/silica composite materials via hydrolysis of titanium(IV) tetra-isopropoxide in sols of spherical silica particles", J. Colloid Interface Sci., 2002, 249, 359-365.

33. Mozia, S., Morawski, A. W., Toyoda, M. and Inagaki, M., "Application of anatase-phase TiO$_2$ for decomposition of azo dye in a photo-catalytic membrane reactor", Desalination, 2009, 241, 97-105.

34. Li, Z., Hou, B., Xu, Y., Wu, D., Sun, Y., Hu, W. and Deng, F., "Comparative study of sol–gel-hydrothermal and sol–gel synthesis of titania–silica composite nanoparticles", J. Solid State Chem., 2005, 178, 1395-1405.

35. Brinker, C. J. and Scherer, G. W., "Sol-gel science: the physics and chemistry of sol-gel processing", Academic Press, INC., San Diego, 1990, 97-228.

36. Kim, K. D., Bae, H. J. and Kim, H. T., "Synthesis and characterization of titania-coated silica fine particles by semi-batch process", Colloids Surf., A: Physicochem. Eng. Asp., 2003, 224, 11-126.

37. Yu, J., Yu, J. C. and Zhao, X., "The effect of SiO$_2$ addition on the grain size and photo-catalytic activity of TiO$_2$ thin films", J. Sol-Gel Sci. Technol., 2002, 24, 95-103.

38. Maia Seco, A., Clara Goncalves, M. and Almeida, R. M., "Densification of hybrid silica–titania sol–gel films studied by ellipsometry and FTIR", Mater. Sci. Eng., 2000, B 76, 193-199.

39. Parks, G. A., "The isoelectric points of solid oxides, solid hydroxides, and aqueous hydroxo complex systems", Chem. Rev., 1965, 65, 177-198.

40. Preoanin, T. and Kallay, N., "Point of zero charge and surface charge density of TiO$_2$ in aqueous electrolyte solution as obtained by potentiometric mass titration", Croat. Chem. Acta, 2006, 79, 95-106.

41. Kosmulski, M., "pH-dependent surface charging and points of zero charge. IV. Update and new

43

approach", J. Colloid Interface Sci., 2009, 337, 439-448.

42. Kosmulski, M., "Chemical properties of material surfaces", CRC Press, 2001, 65-293.

43. Cuddy, M. F., Poda, A. R. and Brantley, L. N., "Determination of isoelectric points and the role of pH for common quartz crystal microbalance sensors", Appl. Mater. Interfaces, 2013, 5, 3514-3518.

44. Ismail, A. A., Ibrahim, I. A., Ahmed, M. S., Mohamed, R. M. and El-Shall, H., "Sol–gel synthesis of titania–silica photo-catalyst for cyanide photo-degradation", J. Photochem. Photobiol., A: Chem., 2004, 163, 445-451.